

## **Smooth mode transfer in AC microgrids during unintentional islanding**

ISSA, Walid <<http://orcid.org/0000-0001-9450-5197>>, EL KHATEB, Ahmad, ANANI, Nader and ABUSARA, Mohammad

Available from Sheffield Hallam University Research Archive (SHURA) at:

<http://shura.shu.ac.uk/16925/>

---

This document is the author deposited version. You are advised to consult the publisher's version if you wish to cite from it.

### **Published version**

ISSA, Walid, EL KHATEB, Ahmad, ANANI, Nader and ABUSARA, Mohammad (2017). Smooth mode transfer in AC microgrids during unintentional islanding. Energy Procedia, 134, 12-20.

---

### **Copyright and re-use policy**

See <http://shura.shu.ac.uk/information.html>

# Smooth mode transfer in AC microgrids during unintentional islanding

Walid Issa<sup>a</sup>, Ahmad El Khateb<sup>b</sup>, Nader Anani<sup>a</sup>, Mohammad Abusara<sup>c</sup>

<sup>a</sup>Sheffield Hallam University, City Campus, Sheffield, S1 1AA, UK

<sup>b</sup>University of Malaya, Kuala Lumpur, Malaysia

<sup>c</sup>University of Exeter, Cornwall Campus, Penryn, TR10 9EZ, UK

---

## Abstract

Microgrid coordinated controllers are designed so as to optimize the utilization of energy available in existing energy storage system (ESS) as well as the energy being generated from prevailing renewable energy sources (RES). If there is a surplus in the generated renewable energy, it will be used to charge the ESS if their capacity permits, otherwise, the surplus energy is curtailed. However, during a grid loss, i.e. during unintentional islanding, the surplus energy can lead to an increase in the DC link voltages feeding the DC-AC inverters, which may subsequently trip them off. Clearly, this has an adverse effect on the reliability of the microgrid. In this paper, a new strategy of microgrid control is proposed for enhancing the microgrid reliability by protecting it against unintentional islanding instability. In this strategy, the DC link voltage is used as a feedback parameter in the droop control loop. This bounds the DC link voltages and consequently leads to reliable operation. The validity of the proposed control scheme was verified by software simulations using MATLAB/Simulink.

© 2017 The Authors. Published by Elsevier Ltd.

Peer-review under responsibility of KES International.

**Keywords:** microgrid; unintentional islanding; DC link voltage; PV; inverters

---

## 1. Introduction

The basic idea of microgrid is to facilitate the distribution of power systems and allows the integration of renewable energy sources into the grid. A microgrid has the ability to connect and disconnect from the grid under certain conditions, e.g. maintenance and intentional/unintentional islanding. A coordinated control scheme is required to transfer microgrid to island mode which is essential to provide accurate power control and seamless integration with the grid.

Droop control is used in microgrids to handle power flow between inverters with total dependency on local measurements [1]–[4]. In unintentional islanding cases, because of the lack of knowledge about the grid status, it could take relatively long time to detect the islanding; the supervisory controller (SC) is unable to update the units about the island mode settings in good time. During that time, a controller is needed to preserve the stability and reliability of each unit in operation until the detection of islanding.

A number of publications have addressed the seamless transfer of microgrids. A nonlinear sliding-mode voltage controller and adaptive power sharing controller are proposed in [5] to achieve seamless mode transfer in microgrids. It employs an internal model voltage controller to mitigate voltage disturbances. However, it does not address the stability of the DC link voltage.

A design of virtual inductance for droop controlled inverters is presented in [6] and virtual resistance in [7] to reduce the inrush current during mode transitions. In [8], the authors focused on achieving seamless transitions from island to grid-connected mode and vice versa by having voltage and current sources working mutually in each mode of operation.

Furthermore, a hierarchical control is proposed in [9] to facilitate the seamless transition between the operating modes (i.e., grid-forming, grid-feeding, and grid-supporting modes). However, all these studies did not address the circulating power during the unintentional islanding and the DC link voltage states stability. In this paper, a DC link voltage loop is proposed for all units to be incorporated with the droop control. This unifies the control schemes for all units and preserves the stability of the DC link

voltage if the grid is lost. Furthermore, it immunizes the microgrid reliability in unintentional islanding cases and provides seamless mode transfer.

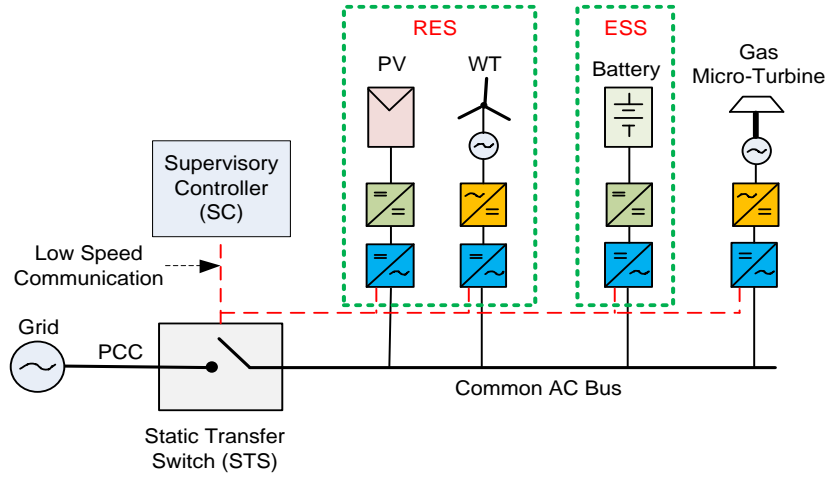


Fig. 1. General microgrid structure [1].

## 2. Energy sources control schemes

The popular power management topology is to set the inverters as AC voltage sources in order to control the output frequency and voltage. The DC-DC converters work as DC voltage sources, i.e. battery, gas micro-turbine or fuel cell followed by buck-boost converter, to control the DC link voltage across the DC link capacitor. The RES modules, PV and wind, inverters, work as AC current sources to generate the available power and to inject it into the grid. The DC-DC converters of the RES are set as DC current sources to inject power into the DC link capacitor. Nevertheless, in this topology, the ESS and RES have different control operation in grid-connected mode and in island mode. In addition, to overcome the circulating power flow during unintentional islanding, it requires an extra DC link voltage loop. The latter loop contains the droop controller, which works intermittently to save any inverter from tripping off [1]. Therefore, there is a need for an outer DC link voltage loop, which contains the droop control loop for reliable operation, in particular, during the unintentional islanding. Thus, in the proposed controller, all units adopt the same control scheme for both modes.

## 3. Circulating power flow

In droop control, different inverters generate different amounts of power as determined by the supervisory controller in grid-connected mode. The output frequency,  $\omega$ , and voltage,  $V$ , from the droop relations are

$$\omega = \omega_o + m(P_{ref} - F(s)P) \quad (1)$$

$$V = V_o + n(Q_{ref} - F(s)Q) \quad (2)$$

where  $m$  and  $n$  are the active and reactive power droop gains,  $P_{ref}$ ,  $Q_{ref}$  are the power references. The averaged power which be calculated after passing the instantaneous power,  $P$ ,  $Q$ , through a low pass filter:

$$F(s) = \frac{1}{\tau s + 1} \quad (3)$$

where  $\tau$  is the filter time constant. When the grid is available, the AC microgrid frequency is dictated by the grid to be  $\omega_{grid}$  which equals the nominal frequency  $\omega_o$  and the three inverters, Fig. 2, generate different power values  $P_1$ ,  $P_2$  and  $P_3$  in grid-connected mode. However, in case of grid loss (unintentional islanding), the bus frequency shifts to a new steady-state value  $\omega_{island}$  according to the DGs power references and loads as calculated in [1] to be

$$\omega_{island} = \omega_o - \frac{m}{2} (P_L - \sum_{i=1}^n P_{i\_ref}) \quad (4)$$

where  $n = 1, 2, \dots$  is the number of inverters. Equation (4) indicates that if the load is more than the sum of power setpoints  $\sum P_{i\_ref}$ , the island frequency will be  $\omega_{island} < \omega_{grid}$  otherwise it will be  $\omega_{island} > \omega_{grid}$ . The latter case results in the power circulating between various units. Those units with lower power will be receiving relatively larger amounts of power resulting in excessive rise in their DC link voltage, which is clearly undesirable as it can cause tripping.

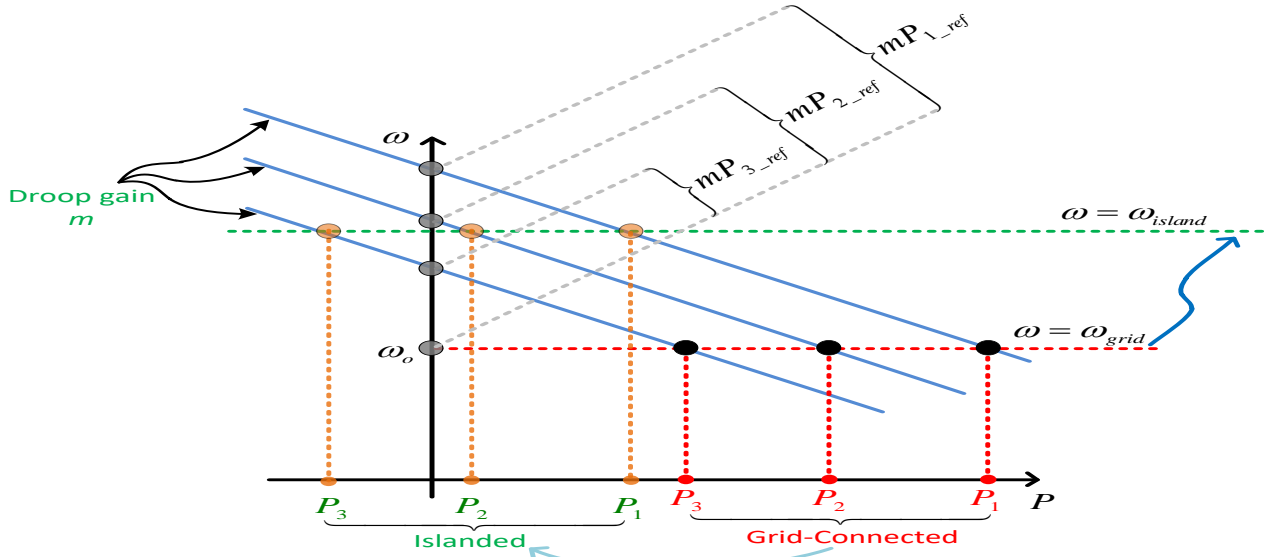


Fig. 2. Frequency droop control operation in unintentional islanding when load is zero

A DC voltage controller with fast response is, therefore, needed to mitigate these DC link voltage disturbances. The buck/boost controller reduces the injected current into the DC link capacitor whenever the DC link voltage rises above a setpoint. Furthermore, the ESS has the ability to reverse the current flow and to switch to charging mode to reduce the voltage rise. However, energy sources such as, RES, gas-turbine and fuel cells, although they can reduce their output current, they are not able to absorb any imported power. Consequently, this imported power will lead to a rise in the DC link voltage which will eventually trip the inverters off.

#### 4. Proposed microgrid control topology

In the microgrid topology proposed in this work, Fig. 3, all energy sources (ESs) are chosen to function as DC current sources. PV and battery-based sources only are considered here. The inverters regulate the DC link voltages and balance the power between the DC and AC sides using a PI controller to dictate the droop control. For PV sources, MPPT (maximum power point tracking) is used to control the output current. The battery power setpoints are received from SC and accordingly it controls the output discharging current or it could be subject to an outer SOC controller. The bandwidth of the PI controllers for output power/frequency regulation in grid-connected/island modes should be lower than the droop loop bandwidth so as to maintain the system stability. Detailed designs of the DC-DC converters control and the droop control have been addressed in the literature for example, [10] and [2].

##### 4.1. MPPT power shifter

During normal grid-connected operation, all of harvested PV power is injected, by the MPPT, into the grid. Nevertheless, the transient circulating grid power during unintentional islanding might pass through the bidirectional PV inverter and charge the capacitor thus increasing its voltage. To prevent such an undesirable increase in the DC link voltage, the MPPT requires an extra loop to monitor the DC link voltage. This allows the MPPT to vary the operating point of the PV system so as to reduce power flowing in to the dc link and thus prevent any unnecessary rise in its voltage as illustrated in Fig. 4.

##### 4.2. ESS control

In grid-connected mode, because the AC bus voltage and frequency are fixed by the grid, in the proposed control scheme of Fig. 3, any DG source, e.g. battery-based unit, must operate as an AC current source. It receives the power reference value from SC by some communication link. The reference value through the power loop (switch a in Fig. 3) controls the DC-DC converter output current, while the DC voltage is fixed by the inverter regulation loop. During normal island mode, the ESS module takes

the master control of the bus frequency and voltage. The reactive power droop control might be used to maintain the AC bus voltage, whilst the active power droop control regulates the DC link voltage and the frequency regulation is implemented by controlling the DC current as in Fig. 3 (switch b).

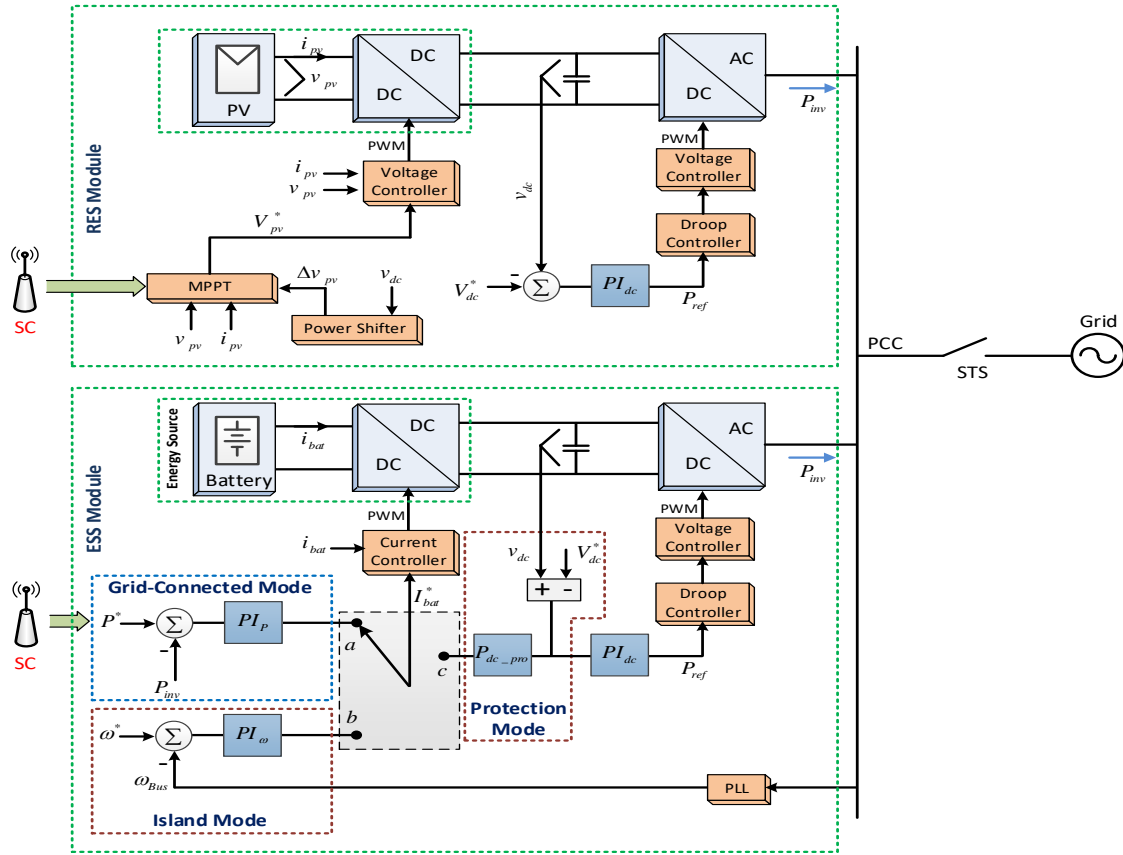


Fig. 3. Proposed microgrid control topology

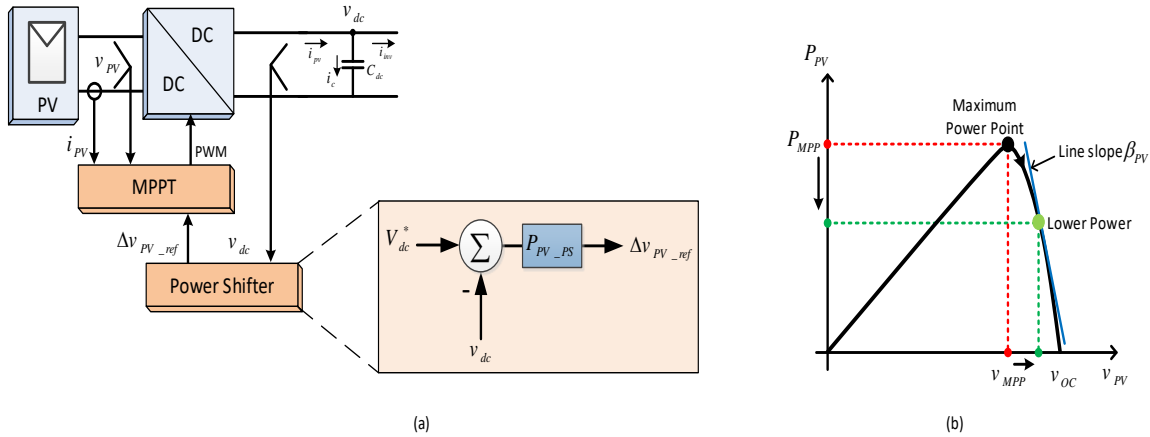


Fig. 4. MPPT Power shifter (a) control loop (b) power curve emulation.

The intentional switching between the two modes has to be done by the SC. However, under unintentional islanding, this suffers from slow response. To eliminate the circulating power and mitigate the risk of any unit trip, this command can be overridden by local protection algorithm (switch c) until the SC updates its settings. Three modes of the ESS module as the ES in grid-connected mode is a current source commanded by the  $P^*$  value from SC. In island mode, the ES is driven locally by the frequency regulation loop. The DC link voltage dictates that dc converter current in the protection mode when  $v_{dc}$  exceeds a defined threshold. It finally dominates the control until getting an update from SC. In all modes, the inverter is a DC voltage source in the DC side and considered as a DC voltage-driven current source in the AC side point of view. It is worth mentioning here that the DC link voltage regulation loop in all units is activated at the time of connecting to the microgrid network after synchronization.

## 5. Simulation results

A two-unit microgrid is simulated in Matlab/Simulink to validate the performance of the proposed control scheme. This microgrid consists of a PV and a battery-based unit. The parameters are listed in Table 1. The performance of the proposed structure has been tested during unintentional islanding scenarios. In grid-connected mode, the PV unit generates its MPPT reference power and the battery unit generates its power reference value sent by SC. The function of the proposed topology against unintentional islanding cases could be assessed by the circulating power figures between the inverters when the grid is lost while  $P_L$  (load power) = 0. Under that condition, the potential scenarios are as follows:

### 5.1. When $P_{Battery} > P_{PV}$

During the time when the PV power is low and/or when the battery power is greater than the PV power, the battery unit discharges its power into the grid. In grid-connected mode, the battery was generating 800 W while the PV power was 400 W. Fig. 5(a) shows the PCC voltage, the inverter's output current and the grid current. At  $t=3$  s, the grid was lost and the power flowed from battery to PV unit. The power shifter operated immediately to reduce this disturbance and to support the inverter's DC voltage regulator. The battery protection mode was activated automatically at  $t=3.05$  s after the DC voltage became greater than the threshold DC voltage  $V_{dcth}$ . At this point the battery was converted to a charging mode absorbing the available PV power and regulated its DC voltage as shown in Fig. 5(b). At  $t=5$  s, the SC detected the islanding then updated the units with the island mode settings at when the frequency regulation loop is on operation. The proposed controller maintained the microgrid stability during such cases and limited the DC link voltages.

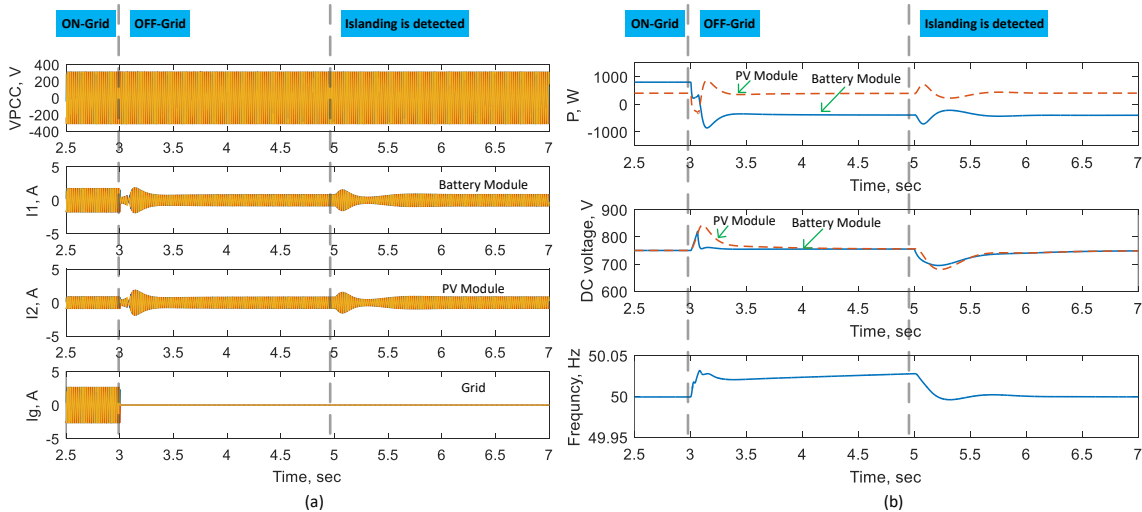


Fig. 5. Simulation results when  $P_{Battery} > P_{PV}$  (a) PCC voltage, inverter's output current and grid current, (b) output active power, DC link voltages of both inverters and the bus frequency.

### 5.2. When $P_{Battery} < P_{PV}$

This scenario presents the case when the PV power is abundant. The PV maximum power was 400 W exported to the grid. The battery was discharging 200 W in grid-connected mode. At  $t=3$  s, the grid was lost and the transient circulating power flowed from PV unit to battery unit as in Fig. 6(a) and trying to charge the battery. However, the control loop of the battery module tried to regulate the output power as its setpoint because islanding has not been detected yet. As a result, the excess power would circulate between the units raising their DC voltages. The PV power shifter acted immediately against this transient by reducing the PV generated power. However, the protection mode in battery module was waiting for the trigger signal when DC voltage becomes  $> 820$  V. At  $t=3.3$  s, the latter was activated automatically and the DC voltage regulation loop is in operation. The DC voltages of the units were settled at 750 V and the circulating power was eliminated as shown in Fig 6(b). Assuming the SC has a maximum of 2 s to detect the islanding, at  $t=5$  s, the SC has updated the units with new settings in island mode and the battery module regulated the bus frequency at 50 Hz. The performance of the new structure limited the instability of the DC link voltages and kept the microgrid serving without interruption.

### 5.3. When battery is charging

This scenario represents the case when the battery is in charging mode or in float ( $P_{ESS} = 0$ ) while the PV power is available. In Fig. 7, the PV power was 400 W exported to the grid. The battery was charging of 200 W in grid-connected mode, i.e. the SOC was low. At  $t=3$  s, the grid was lost and the transient circulating power ran from PV unit to battery unit. The control loop of the battery module tried to regulate the output power as its setpoint before the islanding detection. As a result, the excess power would circulate between the units and consequently raising the DC voltages. The PV power shifter acts immediately against this transient by reducing the PV generated power. However, the DC voltage of the battery unit did not reach the threshold (820 V) and the protection loop was not activated. This reveals that the power shifter action was enough to limit the DC voltages and to eliminate the circulating power. It is assumed that the SC detected the grid loss at  $t=5$  s and updated the units about new settings in island mode. At when the battery regulated the bus frequency at 50 Hz.

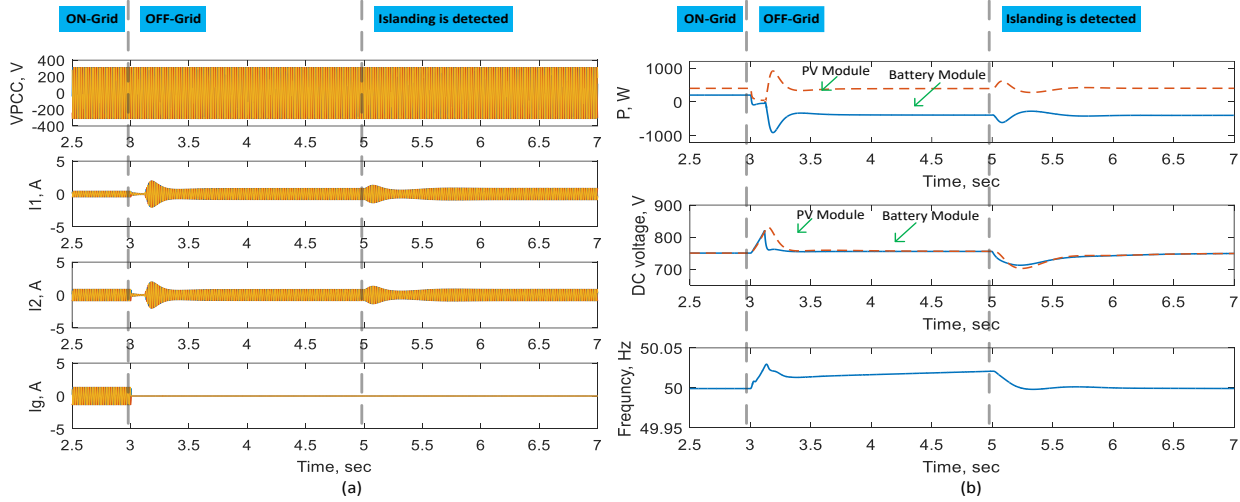


Fig. 6. Simulation results when  $P_{Battery} < P_{PV}$  (a) PCC voltage, inverter's output current and grid current, (b) output active power, DC link voltages of both inverters and the bus frequency.

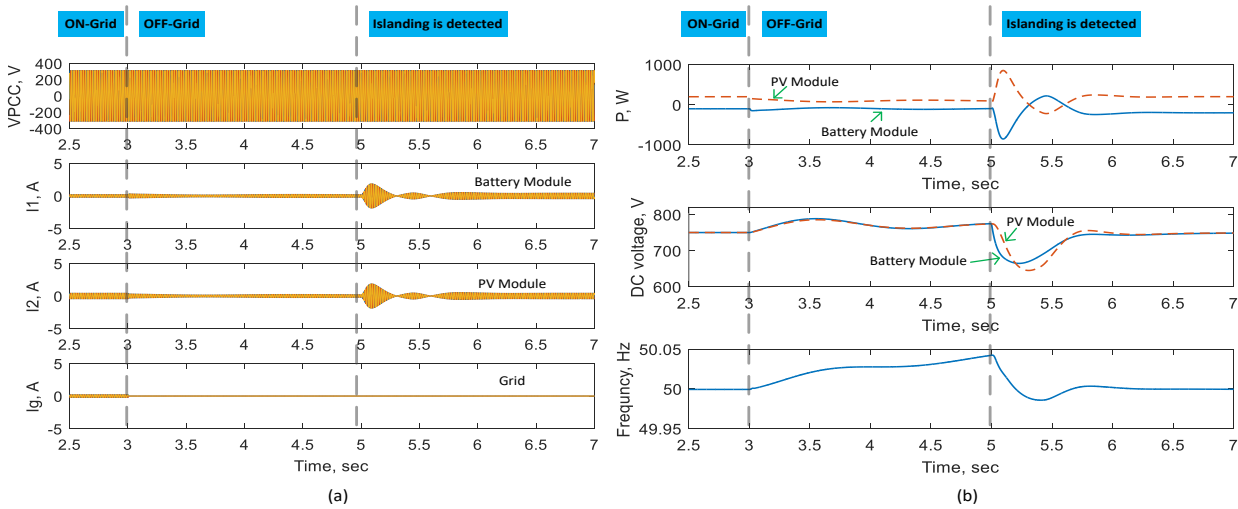


Fig. 7. Simulation results when *Battery* is charging (a) PCC voltage, inverter's output current and grid current, (b) output active power, DC link voltages of both inverters and the bus frequency

## 6. Conclusion

The topology of a new scheme of controlling a microgrid, which uses a battery-based ESS and a PV renewable energy source, has been presented. The ultimate objective of the scheme is to prevent rises in the DC link voltage of the inverters. Furthermore, the proposed scheme results in a unified control structure for all units. The control scheme has been verified using

MATLAB/Simulink simulations. The simulation results indicate good performance of the proposed control scheme as evident by the stability of the microgrid and the seamless transfer of operating mode from grid to island.

Table 1 Simulation setup parameters

Inverter output impedance		ESS power controller	
$X$	$1mH$	$k_{p,p}$	0.001
$R$	$0.08\Omega$	$k_{i,p}$	0.01
DC voltage regulator		ESS frequency regulator	
$k_{p,dc}$	25	$k_{p,\omega}$	10
$k_{i,dc}$	60	$k_{i,\omega}$	25
MPPT shifter		ESS protection loop	
$k_{pv,ps}$	5	$k_{dc,pro}$	0.1
Droop controller		$v_{dc,th}$	820V
$m$	$8.5 \times 10^{-4}$	Output parameters	
$n$	$8.5 \times 10^{-4}$	$V$	220V
$\tau$	$5 \times 10^{-3}$	$\omega$	$2\pi.50$

## References

- [1] Issa W, Abusara M, Sharkh S. Control of Transient Power during Unintentional Islanding of Microgrids. IEEE Transactions on Power Electronics. 2014;30(8):4573 - 84.
- [2] Abusara MA, Sharkh SM, Guerrero JM. Improved droop control strategy for grid-connected inverters. Sustainable Energy, Grids and Networks. 2015;1:10-9.
- [3] Issa W, Abusara M, Sharkh S, Tapas M. A small signal model of an inverter-based microgrid including DC link voltages. 17th European Conference on Power Electronics and Applications; 2015 8-10 Sep 2015; Geneva, Switzerland: EPE 2015.
- [4] Issa W, Sharkh S, Mallick T, Abusara M. Improved Reactive Power Sharing for Parallel-Operated Inverters in Islanded Microgrids. Journal of Power Electronics. 2016.
- [5] Mohamed YARI, Radwan AA. Hierarchical Control System for Robust Microgrid Operation and Seamless Mode Transfer in Active Distribution Systems. IEEE Transactions on Smart Grid. 2011;2(2):352-62.
- [6] Shang-Hung H, Chun-Yi K, Tzung-Lin L, editors. Design of virtual inductance for droop-controlled inverter with seamless transition between islanded and grid-connected operations. IEEE Energy Conversion Congress and Exposition (ECCE), 2012; 2012 15-20 Sept. 2012.
- [7] Josep M. Guerrero NB, José Matas, Luis García de Vicuña, Jaume Miret. Decentralized Control for Parallel Operation of Distributed Generation Inverters in Microgrids Using Resistive Output Impedance. IEEE Industrial Electronics. 2006.
- [8] Micallef A, Apap M, Spiteri-Staines C, Guerrero JM. Single-Phase Microgrid With Seamless Transition Capabilities Between Modes of Operation. IEEE Transactions on Smart Grid. 2015;6(6):2736-45.
- [9] Wang J, Chang NCP, Feng X, Monti A. Design of a Generalized Control Algorithm for Parallel Inverters for Smooth Microgrid Transition Operation. IEEE Transactions on Industrial Electronics. 2015;62(8):4900-14.
- [10] Mahmood H, Michaelson D, and J. Jin. Control strategy for a standalone PV/battery hybrid system, in 38th Annual Conference on IEEE Industrial Electronics Society -IECON 2012 2012, pp. 3412-3418